NANO LETTERS

2008
Vol. 8, No. 6
1683-1688

Ionic Effects on the Equilibrium Dynamics of DNA Confined in Nanoslits

Chih-Chen Hsieh, Anthony Balducci, and Patrick S. Doyle*

Department of Chemical Engineering, Massachusetts Institute of Technology, 77 Massachusetts Avenue, Cambridge, Massachusetts 02139

Received February 28, 2008; Revised Manuscript Received April 2, 2008

ABSTRACT

The ionic effects on the dynamics and conformation of DNA in silt-like confinement are investigated. Confined λ-DNA is considered as a model polyelectrolyte, and its longest relaxation time, diffusivity, and size are measured at a physiological ionic strength between 1.7−170 mM. DNA properties change drastically in response to the varying ionic environment, and these changes can be explained by blob theory with an electrostatically mediated effective diameter and persistence length. In the ionic range we investigate, the effective diameter of DNA that represents the electrostatic repulsion between remote segments is found to be the main driving force for the observed change in DNA properties. Our results are useful for understanding the manipulation of biomolecules in nanofluidic devices.

With the advance of nanotechnology, new devices have been created to manipulate biomolecules. Many such applications, including DNA separation[1] and gene mapping,[2] rely on the confinement-induced change in molecular properties. Several studies have been devoted to the investigation of those confinement effects on DNA and have had fruitful progress.[3–6] On the other hand, the ionic environment is also known to have a strong influence on biomolecule properties and can be readily manipulated in experiments. However, the compound effects of confinement and ionic environment, critical for many applications, are yet to be fully understood.

Several studies have investigated the ionic effects on confined DNA conformation in rectangular channels (height (h) ≈ width (d)).[2,7,8] DNA extension was found to increase with decreasing ionic strength. This observation was explained either by de Gennes' blob theory (h and $d > p$ (persistence length))[9,10] or by Odijk's deflection chain theory (h and $d < p$).[11] Although the finding is promising, we find that the buffer ionic strengths reported in these studies are somewhat inaccurate especially at low salt concentration due to neglect of the ionic contribution of antiphotobleaching agents. Furthermore, it is not clear how ionic environment will influence DNA dynamics and whether the above theories can be applied. In the current study, we investigate the ionic effects on both conformation and dynamics of DNA confined in nanoslits with better control on buffer ionic strength. We show that our analysis can be used to explain the ionic effects on both confined and unconfined DNA, providing a consistent picture for this highly debated issue of DNA/polyelectrolytes.

To understand the physical origin of the ionic effects on polyelectrolytes, we first consider the conformation of neutral polymers. From the Flory theory,[12] the equilibrium size (R_{bulk}) of an unconfined, semiflexible polymer in good solvents can be expressed as:

$$R_{bulk} \sim v^{1/5} p^{2/5} N^{3/5} \sim L^{3/5} (pw)^{1/5} \quad (1)$$

where $N$is the total number of statistical segments, p is the persistence length representing the short-ranged stiffness of the chain, w is the effective diameter of the polymer, $v \approx wp^2$ is the long-ranged excluded volume (EV) of a statistical segment, and $L = 2pN$ is the contour length. When such a molecule is confined in a slit geometry with $p < h < R_{bulk}$, blob theory[9,10] assumes that it behaves like a string of blobs with each blob having a diameter h and g statistical segments. g can be estimated by setting R_{bulk} in eq 1 equal to h/2, and therefore $g \sim h^{5/3} w^{-1/3} p^{-4/3}$. Blob theory further assumes that the blobs follow a two-dimensional (2D) self-avoiding walk. Consequently, the scaling of the nominal size (R_{slit}) of the confined chain can be obtained:

$$R_{slit}^2 \sim (h(N/g)^{3/4})^2 \sim L^{3/2} h^{-1/2} (pw)^{1/2} \quad (2)$$

By assuming that hydrodynamic interactions are screened between blobs and that the drag acting on a blob is proportional to its size, the drag coefficient of a chain ζ_{chain} can be estimated as $\zeta_{chain} \sim \eta L h^{-2/3} (pw)^{1/3}$. Here, η is the solvent viscosity. The longest relaxation time τ_1 and the diffusivity D can be subsequently derived:

* Corresponding author. E-mail: pdoyle@mit.edu.

10.1021/nl080605+ CCC: $40.75
Published on Web 05/07/2008

$$D \sim \frac{k_B T}{\zeta_{chain}} \sim \eta^{-1} L^{-1} h^{2/3} (pw)^{-1/3} \quad (3)$$

$$\tau_1 \sim R_{slit}^2 \zeta_{chain} \sim \eta L^{5/2} h^{-7/6} (pw)^{5/6} \quad (4)$$

The assumptions made in the blob theory have been examined experimentally using DNA at a constant ionic strength.[5] Only the assumption of nondraining blob was found compromised, and this leads to deviations in the predicted h dependence of eqs 3 and 4. Since the remaining assumptions have been verified, eq 2 and the scalings in eqs 3 and 4 related to L and (pw) are valid.

For polyelectrolytes, Coulombic interactions introduce a new length scale (Debye screening length, κ^{-1}) to the molecule and give rise to both local and nonlocal effects.[13] The former results in an increase of chain stiffness, and the latter resembles an excluded volume between chain segments. Therefore, a polyelectrolyte can be considered as a neutral polymer with its p and w having an electrostatic contribution depending on the ionic environment.

A theoretical prediction of the electrostatically mediated effective diameter of DNA has been given by Stigter.[14] He estimated w of DNA molecules by matching the second virial coefficient of a dilute solution containing charged rod with finite ionic strength to that of the same solution containing neutral rods with a known diameter. The effective diameter of DNA was shown to follow:[14,15]

$$w = \kappa^{-1}\left(0.7704 + \log \frac{2\pi\nu_{eff}^2}{k_B T \varepsilon \varepsilon_0 \kappa}\right) \quad (5)$$

where ν_{eff} is an effective DNA line charge, ε is the dielectric constant of water, ε_0 is the permittivity of free space, and κ is the inverse Debye screening length [$\kappa^2 = (2N_A e^2 I)/(\varepsilon_0 \varepsilon k_B T)$; N_A is Avogadro's number; e is the electronic charge; I is the ionic strength; k_B is Boltzmann's constant, and T is the absolute temperature]. We note that ν_{eff} is not the true line charge ν_0 but a function of ν_0, the intrinsic diameter of DNA and ionic strength. ν_{eff} was introduced so that w calculated numerically with the Poisson−Boltzmann equation can be expressed in a simple form derived using Debye−Hückel approximation.[14] Stigter assumed that the intrinsic radius of DNA is 1.2 nm and each phosphate group carries −0.73e. He found w not very sensitive to these values. This prediction of w has been verified by various studies using sedimentation,[16] osmotic pressure,[17] and measurement of the probability of trefoil knots of DNA during cyclization.[18,19]

The most well-known analytical prediction of the electrostatic persistence length (p_{el}) of a semiflexible chain was given by Odijk,[20] and Skolnick and Fixman[21] (OSF). They estimated p_{el} by including the short-ranged electrostatic potential to the effective bending energy of a weakly deformed semiflexible polyelectrolyte. The persistence length was expressed as the sum of the intrinsic persistence length p_0 and the electrostatic persistence length. For DNA, a quantitative prediction was given as:

$$p = p_0 + p_{el} = p_0 + \frac{\xi^2}{4\kappa^2 l_B} = p_0 + \frac{0.0324M}{I} nm \quad (6)$$

where l_B is the Bjerrum length (about 0.72 nm in aqueous solution at room temperature), and ξ is the Manning parameter defined as the ratio of l_B over the effective charge distance on the chain. The last part of eq 6 is only valid for strongly charged polyelectrolytes with $\xi > 1$, such as DNA. For $\xi > 1$, counterions condense on the chain and reduce the charge density along the chain to make $\xi = 1$.[22] The most significant prediction of OSF theory was $p_{el} \sim \kappa^{-2}$. Baumann et al.[23] have shown experimentally that the measured electrostatic persistence length agrees quantitatively with the OSF prediction and have found p_0 to be 50 nm for unstained DNA, consistent with other studies.[24]

However, OSF theory has been challenged by many studies. Several experiments investigating the electrostatic persistence length of semiflexible polyelectrolytes reported $p_{el} \sim \kappa^{-1}$.[25–27] Some theoretical studies have argued that the observed linear dependence is the behavior of polyelectrolytes that follow $p_{el} \sim \kappa^{-2}$ with an excluded volume described by $w \sim \kappa^{-1}$.[28,29] Dobrynin[30] pointed out that OSF theory was incorrect because the torsional angle between successive bonds was implicitly fixed in the derivation. If this constraint is removed, $p_{el} \sim \kappa^{-1}$ is obtained. Dobrynin[31] performed a regression to the experimental results of Porschke[26] and Baumann et al.[23] and provided an empirical formula of the electrostatic persistence length of DNA:

$$p = p_0 + p_{el} = 46.1 + \frac{1.9195M}{\sqrt{I}} nm \quad (7)$$

We compare the Debye screening length, the predicted effective diameter, the predicted persistence length of DNA with OSF theory, and the empirical persistence length of DNA fit by Dobrynin at different ionic strengths in Figure 1. Although the persistence lengths given by the OSF theory and the empirical fitting follow distinct scalings at very low ionic strength, they are similar and depend very weakly on I for $I > 1mM$. On the other hand, the effective diameter of DNA depends strongly on I even at $I \approx 0.5M$. Therefore, it is expected that the ionic effects on DNA will be dominated by the change in the effective diameter for $0.5M > I > 1mM$.

The nanoslits were made in glass using the method developed by Mao and Han.[32] The slits are 450 nm high and 150 μm wide. The height was determined from SEM images. λ-DNA (48.5 kbp) were purchased from New England Biolabs (NEB). DNA samples were stained with YOYO-1 fluorescent dye (Invitrogen) at 50 °C for one hour at a concentration of 1 dye every 4 base pairs. The experimental buffers are 0.02×, 0.1×, 0.5×, 2×, and 5× TBE solutions diluted from 5× TBE made with 0.45 M Tris base, 0.45 M boric acid, and 0.01 M EDTA. To slow photobleaching and photobleakage of stained DNA, a radical scavenger of 0.5% (v/v) β-mercaptoethanol (CabioChem) and an oxygen scavenger system consisting of 7.26 mg/ml β-D glucose, 0.37 μl/ml catalase (Roche), and 0.16 mg/ml glucose oxidase (Roche) were included in the buffer solutions. Nanoslits were filled the night before experiments with corresponding TBE buffers and flushed by an electro-osmosis

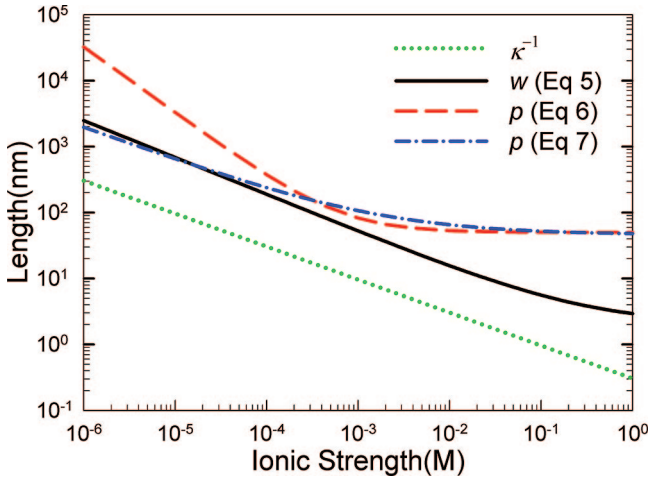

Figure 1. Debye length (dotted line), the predicted effective diameter of DNA (eq 5, solid line), the predicted persistence length of OSF theory (eq 6, dashed line), and the empirical persistence length (eq 7, dashed-dotted line) versus ionic strength.

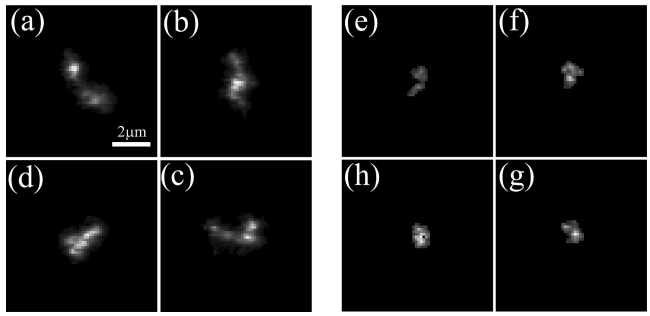

Figure 2. Time-sequence images of λ-DNA confined in a 450 nm high slit in 0.02× TBE (a−d) and in 2× TBE (e−h). Successive frames are separated by one longest relaxation time.

flow at a field of 10 V/cm to remove bubbles. DNA were driven into the channel using an electric field of 10−30 V/cm, depending on the DNA mobility. Single DNA molecules were observed with an inverted Zeiss Axiovert 200 microscope with a Plan-Apochromat 100× (N.A. 1.40) oil-immersed objective. The images were taken with a Hamamatsu EB-CCD camera (model: 7190−21) at a rate of 30 frames/sec. Averages were taken over ensembles of 20∼35 molecules. DNA diffusivity was obtained from the slope of the averaged mean-square displacement of the center of the mass of DNA versus lag time. The longest relaxation time was extracted from the rate of decay of the autocorrelation function of DNA orientation. The image processing and data analysis are the same as described in Hsieh et al.[5] Figure 2 shows time-sequence images of confined λ-DNA in 0.02× TBE (a−d) and in 5× TBE (e−h).

The antiphotobleaching and oxygen scavenger agents have been used in many single-molecule studies to prolong the observation time of stained DNA.[3,7,33] However, their effects on buffer ionic strength have not been fully recognized even in recent studies focusing on ionic effects on DNA behavior.[2,7] We point out that β-mercaptoethanol (BME) is a weak acid ($pK_a = 9.6$). Moreover, the oxygen scavenger system produces gluconic acid ($pK_a = 3.6$) as a final product. Both agents lead to an increase of buffer ionic strength and a decrease of buffer pH, which can be overwhelming in a weak buffer. If oxygen is not blocked from the experimental system, the accumulating gluconic acid can reduce the pH of a 0.02× TBE buffer from 8 to about 4 in 30 min and eventually results in DNA condensation. Even a less significant decrease in system pH may alter the DNA properties by reducing its charge density. To prevent oxygen from permeating the experimental system, we sealed the nanochannels in a chamber purged continuously by nitrogen that has been presaturated by the same buffer. The experimental setup has been tested using 0.02× TBE, and the system pH has decreased by only 0.3 over a typical experimental time course of 4 h, representing a mere 3×10^{-4} M increase in the ionic strength. Because the ionic strength increase due to the gluconic acid generated during the experiments should be independent of the buffer concentration, the ionic strength can be considered constant in experiments with higher concentration of TBE buffers.

The buffer ionic strength is defined by $I = 1/2\sum c_i z_i^2$ where c_i and z_i are the molar concentration and the charge of ith ion, respectively. The ion concentration of different species are evaluated by solving iteratively the system chemical equilibria. We have used the pK_b of Tris base (5.94), the pK_a of boric acid (9.24) and ETDA (1.99, 2.67, 6.16, 10.26), and the pK_w of water (14). The calculation also considers the free radical scavenger BME as an weak acid ($pK_a = 9.6$).[7] All pKs were determined at 25 °C at ideal conditions. To include the nonideality of ions at high I, we estimate the activity coefficients of ions using the Davies equation[34] and make corresponding corrections in the calculation. The ionic strength and pH of experimental TBE buffers are listed in Table 1. As can be seen, BME has strong influence on system ionic strength and pH. We also estimate the ionic contribution (I_M) from macro-ions (glucose oxidase and catalase) using Linderstrerm-Lang approximation ($I_M = 1/2\sum c_i|z_i|$)[35,36] and find I_M negligible in our system. The predicted pH of TBE solutions are found very close to the measured ones, and the predicted ionic strengths compare well with those reported by Reisner et al.[7]

Figure 3 shows the ionic effects on the dynamics and conformation of confined λ-DNA. It is important to notice that the buffer viscosity η is not a constant but increases with TBE concentration. Therefore, the true ionic effects on any dynamic properties can only be recovered when the change of viscosity is offset. The viscosities of experimental buffers were determined at 26 °C by measuring the diffusivity of 0.748 μm polystyrene beads (Polysciences).[37] We find the viscosity of 5×, 2×, 0.5×, 0.1×, and 0.02× TBE with 0.5% BME to be 1.18, 1.04, 0.93, 0.93, and 0.92 cP, respectively. To remove viscosity effects from the data, we define a scaled diffusivity $D' = (D\eta/\eta_{ref})$ and a scaled relaxation time $\tau_1' = (\tau_1\eta_{ref}/\eta)$ where the reference viscosity (η_{ref}) is taken to be 1 cp.

To proceed with the discussion, we first describe the fitting scheme used in Figure 3. For each plot, the three curves represent fittings of the corresponding theoretical scalings (eqs 3, 4, 2) with different expressions for p on I. The solid, dashed, and dashed-dotted curves are the fittings with p

Table 1. Comparison of Calculated Ionic Strength (I) and pH of TBE Buffers

buffer	5×	2×	0.5×	0.1×	0.02×
$I(M)$	1.65×10^{-1}	6.26×10^{-2}	1.48×10^{-2}	2.86×10^{-3}	5.68×10^{-4}
I (with 0.5%BME)(M)	1.70×10^{-1}	6.66×10^{-2}	1.79×10^{-2}	4.70×10^{-3}	1.34×10^{-3}
pH	8.44	8.48	8.51	8.54	8.54
pH (with 0.5%BME)	8.42	8.43	8.37	8.14	7.74

described as a constant, by eq 6 and by eq 7, respectively. w is estimated using eq 5 for all fittings because its validity has been widely accepted. Only one proportionality constant was used in each fitting. As a result, the shape of the curves was independent of the proportionality constant but was determined a priori by the blob theory with the predicted formula for DNA persistence length and effective width. We fit to the four data points at highest ionic strength so that the relatively weak contribution to DNA properties from the change of p can be distinguished at the lowest ionic strength.

In Figure 3a, D' is shown to approximately double when I increases from 1.7 mM to 170 mM. The results indicate that electrostatic screening becomes stronger with increasing ionic strength, resulting in a reduction of the size and therefore of the drag of the DNA. We fit the scaling of eq 3 to the experimental results. All three curves are in fair agreement with the experimental results, implying that the ionic effect on w dominates the observed change in DNA diffusivity in this range of I.

Figure 3b shows that the longest relaxation time increases approximately 4 times in response to the change of I from 170 mM to 1.7 mM. The scaling of eq 4 is fit to the experimental results. For $I \geq 5mM$, all three curves are very close to each other and are in excellent agreement with experimental results. For $I < 5mM$, the dashed and dashed-dotted lines deviate from the solid curve, showing that p_{el} becomes significant relative to p_0. The experimental data at the lowest I lies between the solid curve and the dashed and dashed-dotted curves. The insets in Figure 3a,b show the diffusivity and the longest relaxation before (open symbols) and after (solid symbols) the viscosity adjustment. The significance of this correction is greatly exemplified by the diffusivity of DNA in 5× TBE buffers. Failure to account for the viscosity change will lead to a very different result.

Figure 3c shows the quantity of $D'\tau'_1 = D\tau_1$ as a function of I. We notice that the product of D and τ_1 is proportional to R_{slit}^2 and using this relationship yields more accurate results than those obtained from image analysis.[5] The equilibrium size of DNA grows with decreasing I, consistent with the findings of earlier studies.[7,2,8] The agreement between experimental results and fitting curves is good and is very similar to that seen in Figure 3b. The experimental data at the lowest ionic strength lies between the solid curve and the dashed and dashed-dotted curves. To summarize the results in Figure 3, we find that the change of DNA dynamic and conformational properties can be described by the blob theory with an electrostatically mediated persistence length and width. More importantly, the observed change in DNA properties due to ionic strength is mainly driven by the change of effective DNA diameter for $I > 1mM$.[7] Since the ionic effect on persistence length is weak for $I > 1mM$, we are unable to determine the true dependence of p_{el} on Debye screening length using our results.

In a recent study, Makita et al.[38] measured the equilibrium size of unconfined T4 DNA at $10^{-6}M \leq I \leq 3M$, covering

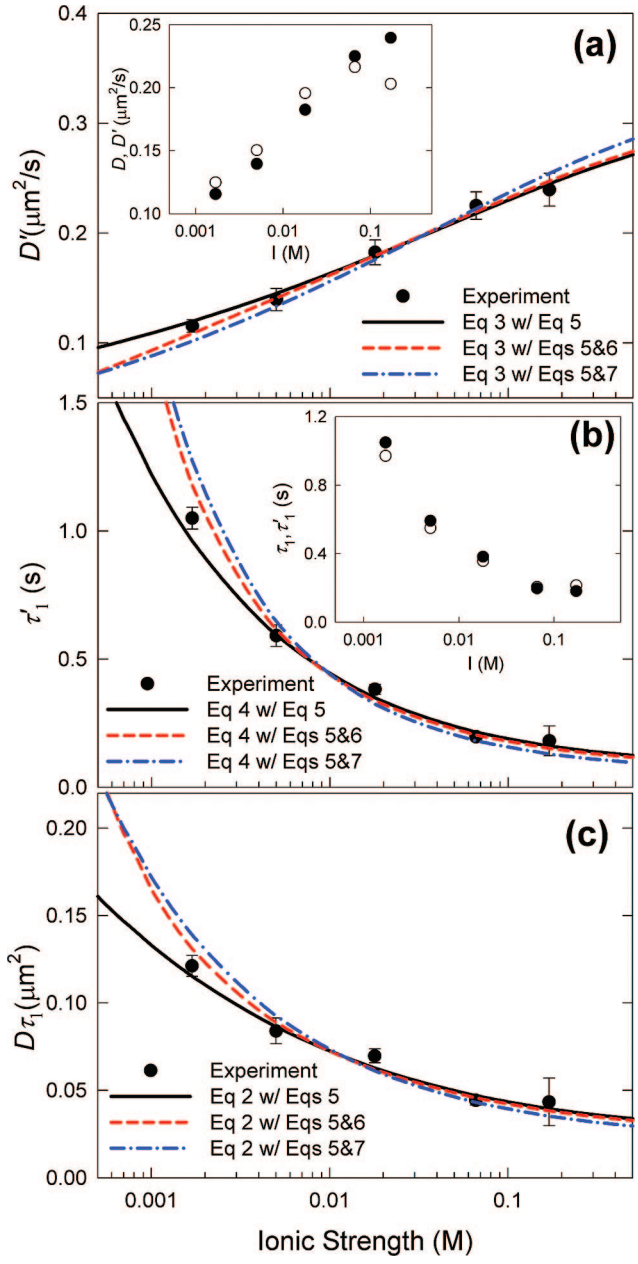

Figure 3. λ-DNA (a) diffusivity, (b) relaxation time, and (c) size as functions of ionic strength. Equations 3, 4, and 2 are fit to DNA diffusivity, relaxation time, and size, respectively. The solid, dashed, and dashed-dotted curves are the fittings with p described as a constant, by eq 6, and by eq 7, respectively. w is estimated using eq 5 for all fittings. The insets in a and b: The measured diffusivity and longest relaxation time before (open symbols) and after (solid symbols) viscosity adjustment.

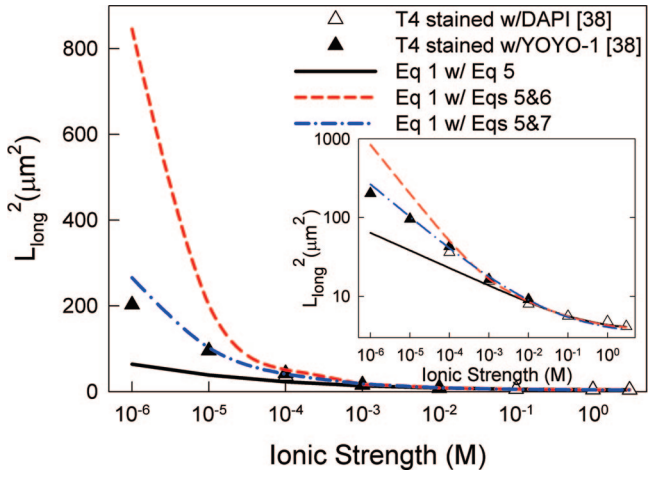

Figure 4. Comparison of DNA conformation measured by Makita et al.[38] with the predicted scaling given in eq 1. The open symbols represent that DNA were stained with DAPI, and the solid ones were stained with YOYO-1. The solid, dashed, and dashed-dotted curves are the fittings with p described as a constant, by eq 6 and by eq 7, respectively. w is estimated using eq 5 for all fittings. The inset plot is the same plot on a log−log scale.

regions where both w and p depend strongly on I . Using the formula of equilibrium size for a worm-like chain in theta solvent, they obtained an effective persistence length that depends linearly on κ^{-1}. Their effective persistence length lumps both local stiffening and nonlocal EV effects of Coulombic interactions and therefore does not provide clear information on exactly how ionic environment affects DNA properties. Given the results of the current study, it is more profound to check if their observation of DNA conformation can be correctly described by eq 1. More importantly, since we have separated local stiffening and nonlocal EV in our analysis, we are capable to examine the dependence of p_{el} using their results.

Figure 4 shows the fits of eq 1 to the measured long-axis length square ($L_{long}^2 \sim R_{bulk}^2$) of T4 DNA reported by Makita et al. The fitting scheme and display of the fitting results are the same as those used in Figure 3. The open triangles represent that DNA were stained with DAPI, and the solid ones were stained with YOYO-1. Only the data obtained at $I > 1mM$ and with DAPI are used in the fittings. Despite the use of different expressions for p, all three curves agree very well with the experimental observation for $I > 1mM$ where the change of w dominates the change of DNA configuration. This agreement demonstrates that our results are consistent with theirs, and the blob theory is valid to interconnect the bulk and confined polymer/polyelectrolyte properties. For $I \leq 1mM$, the experimental results are in excellent agreement with the dashed-dotted curve that uses p given by eq 7, strongly suggesting $p_{el} \sim \kappa^{-1}$.

To finish the discussion we remark that the interplay between the ionic environment and the negatively charged glass channel can induce other effects on DNA that are not considered in the current study. For example, as a channel becomes smaller or the ionic strength becomes lower so that $h\kappa \approx O(1)$, one will expect a reduction in the effective dimension of the confinement due to the coion depletion near the boundary. Also at the same limit, electroneutrality will lead to an enrichment of the counterions in nanochannels, and charge regulation could occur on the surfaces of DNA and the channel.[39] These phenomena can cause opposite effects on DNA behavior and can be difficult to isolate. However, they are expected to have a negligible influence in the current study since the largest Debye screening length is less than 8 nm, about 1.7% of the height of the nanoslits. Nevertheless, the current analysis that relates confined polyelectrolyte behavior to the ionic environment (eqs 2, 3, 4) should still be sound as long as the corresponding adjustments are made to h, w, and p to account for these effects.

Practically, our results can be useful for applications using confinement as a means to manipulate biomolecules. For example, modulating ionic strength could improve the speed and resolution of entropic trapping devices[1] and DNA prisms.[40] In addition, the strong ionic effects on DNA properties suggest that the ion enrichment and depletion in nanochannels[41] should be considered as an important factor that can drastically affect the properties of biomolecules and may be exploited for new applications.

Acknowledgment. The authors thank U.S. Genomics and NSF Career Grant CTS-0239012 for funding.

References

(1) Han, J.; Craighead, H. G. *Science* **2000**, *288*, 1026.
(2) Jo, K.; Dhingra, D. M.; Odijk, T.; de Pablo, J. J.; Graham, M. D.; Runnheim, R.; Forrest, D.; Schwartz, D. C. *Proc. Nat. Acad. Sci.* **2007**, *104*, 2673.
(3) Reisner, W.; Morton, K. J.; Riehn, R.; Wang, Y. M.; Yu, Z.; Rosen, M.; Sturm, J. C.; Chou, S. Y.; Frey, E.; Austin, R. H. *Phys. Rev. Lett.* **2005**, *94*, 196101.
(4) Balducci, A.; Mao, P.; Han, J.; Doyle, P. S. *Macromol.* **2006**, *39*, 6273.
(5) Hsieh, C. C.; Balducci, A.; Doyle, P. S. *Macromol.* **2007**, *40*, 5196.
(6) Balducci, A.; Hsieh, C. C.; Doyle, P. S. *Phys. Rev. Lett.* **2007**, *99*, 4.
(7) Reisner, R.; Beech, J. P.; Larsen, N. B.; Flyvbjerg, H.; Kristensen, A.; Tegenfeldt, J. O. *Phys. Rev. Lett.* **2007**, *99*, 058302.
(8) Krishnan, M.; Monch, I.; Schwille, P. *Nano Lett.* **2007**, *7*, 1270.
(9) Brochard, F.; de Gennes, P. G. *J. Chem. Phys.* **1977**, *67*, 52.
(10) Daoud, M.; de Gennes, P. G. *J. Phys.(Paris)* **1977**, *38*, 85.
(11) Odijk, T. *Macromol.* **1983**, *16*, 1340.
(12) Rubinstein, M.; Colby, R. H., *Polymer Physics*, Oxford University Press, New York 2003.
(13) Odijk, T.; Houwaart, A. C. *J. Polym. Sci. B Polym. Phys.* **1978**, *16*, 627.
(14) Stigter, D. *Biopolymers* **1977**, *16*, 1435.
(15) Stigter, D. *J. Colloid Interface Sci.* **1975**, *53*, 296.
(16) Brian, A. A.; Frisch, H. L.; Lerman, L. S. *Biopolymers* **1981**, *20*, 1305.
(17) Yarmola, E. G.; Zarudnaya, M. I.; Lazurkin, Y. S. *Journal of Biomolecular Structure and Dynamics* **1985**, *2*, 981.
(18) Shaw, S. Y.; Wang, J. C. *Science* **1993**, *260*, 533.
(19) Rybenkov, V. V.; Cozzarelli, N. R.; Vologodskii, A. V. *Proc. Natl. Acad. Sci.* **1993**, *90*, 5307.
(20) Odijk, T. *J. Polym. Sci. B Polym. Phys.* **1977**, *15*, 477.
(21) Skolnick, J.; Fixman, M. *Macromol.* **1977**, *10*, 944.
(22) Manning, G. S. *J. Chem. Phys.* **1969**, *51*, 924.
(23) Baumann, C. G.; Smith, S. B.; Bloomfield, V. A.; Bustamante, C. *Proc. Natl. Acad. Sci.* **1997**, *94*, 6185.
(24) Hagerman, P. J. *Annu. Rev. Biophys. Biophys. Chem.* **1988**, *17*, 265.
(25) Geller, K. *Studia Biophysica* **1982**, *87*, 231.
(26) Porschke, D. *Biophys. Chem.* **1991**, *40*, 169.
(27) de Nooy, A. E. J.; Besemer, A. C.; vanBekkum, H.; vanDijk, J.; Smit, J. A. M. *Macromol.* **1996**, *29*, 6541.
(28) Everaers, R.; Milchev, A.; Yamakov, V. *Euro. Phys. J. E* **2002**, *8*, 3.
(29) Ullner, M. *J. Phys. Chem. B* **2003**, *107*, 8097.
(30) Dobrynin, A. V. *Macromol.* **2005**, *38*, 9304.

(31) Dobrynin, A. V. *Macromol.* **2006**, *39*, 9519.
(32) Mao, P.; Han, J. *Lab Chip* **2005**, *5*, 837.
(33) Perkins, T. T.; Smith, D. E.; Chu, S. *Science* **1997**, 276–2016.
(34) Butler, J. N.; Cogley, D. R., *Ionic Equilibrium: Solubility and pH Calculations*, John Wiley and Sons, New York 1998.
(35) Linderstrom-Lang, K. *Trans. Faraday Soc.* **1935**, *31*, 324.
(36) Rible, H., *pH and Buffer Theory - A New Approach*, John Wiley and Sons, Chichester, England 1996.
(37) Savin, T.; Doyle, P. S. *Biophys. J.* **2005**, *88*, 623.
(38) Makita, N.; Ullner, M.; Yoshikawa, K. *Macromol.* **2006**, *39*, 6200.
(39) Israelachvili, J. N., *Intermolecular and surface forces*, Academic Press, London 1991.
(40) Huang, L. R.; Silberzan, P.; Tegenfeldt, J. O.; Cox, E. C.; Sturm, J. C.; Austin, R. H.; Craighead, H. *Phys. Rev. Lett.* **2002**, *89*, 4.
(41) Kim, S. J.; Wang, Y. C.; Lee, J. H.; Jang, H.; Han, J. *Phys. Rev. Lett.* **2007**, *99*, 044501.

NL080605+